

Experimental Demonstration of a Controlled-NOT Wave-Packet Gate

B. DeMarco, A. Ben-Kish,* D. Leibfried, V. Meyer, M. Rowe,† B. M. Jelenković,‡ W. M. Itano, J. Britton, C. Langer, T. Rosenband, and D. J. Wineland

NIST, Time and Frequency Division, Ion Storage Group, Boulder, Colorado 80305

(Received 20 August 2002; published 9 December 2002)

We report the experimental demonstration of a controlled-NOT (CNOT) quantum logic gate between motional and internal-state qubits of a single ion where, as opposed to previously demonstrated gates, the conditional dynamics depends on the extent of the ion's wave packet. Advantages of this CNOT gate over one demonstrated previously are its immunity from Stark shifts due to off-resonant couplings and the fact that an auxiliary internal level is not required. We characterize the gate logic through measurements of the postgate ion state populations for both logic basis and superposition input states, and we demonstrate the gate coherence via an interferometric measurement.

DOI: 10.1103/PhysRevLett.89.267901

PACS numbers: 03.67.Lx, 32.80.Qk

Considerable attention is now focused on developing quantum computer technology across a diverse set of physical systems [1,2]. Using laser cooled trapped atomic ions for quantum computing and information processing [3] carries many advantages as most of the basic building blocks of quantum computing have been demonstrated, including high efficiency state initialization and readout [4–9], entangling gates [10,11], individual addressing [8], and long qubit coherence times [9,12]. Areas of concentration for current work with trapped ions include simplifying quantum logic operations and increasing their fidelity, as well as scaling up the complexity of computations [13–15]. Here we report the experimental demonstration of a CNOT logic gate between motional and internal-state qubits of a trapped ${}^9\text{Be}^+$ ion that requires fewer resources than that of Ref. [10]. This gate is fundamentally different from previously demonstrated gates in that the conditional dynamics depend on the size of the atomic wave packet compared to the wavelength of the applied radiation [16].

The quantum CNOT logic gate between two qubits has become a paradigm for quantum computing because universal quantum computation can be carried out with the CNOT gate and single qubit rotations [1]. A CNOT gate toggles the state of a target qubit depending on the state of a control qubit. If the logic basis states are labeled as $|0\rangle$ and $|1\rangle$, then the general target state $\cos(\theta)|0\rangle + e^{i\phi}\sin(\theta)|1\rangle$ should be unaffected if the control qubit is in the $|0\rangle$ state and transformed to $\cos(\theta)|1\rangle + e^{i\phi}\sin(\theta)|0\rangle$ for a $|1\rangle$ control qubit. Here θ and ϕ are taken to be arbitrary angles to designate the most general superposition state. Based on a previous proposal [16], we demonstrate a CNOT gate in the trapped ion system that requires only a single laser pulse and no auxiliary levels, and is therefore simplified compared to a previous implementation that required three laser pulses and an auxiliary internal state [10]. Furthermore, the method employed here is free from level shifts introduced by the gate coupling.

The qubits in our implementation of the CNOT gate are spanned by the internal and motional levels of a single trapped ${}^9\text{Be}^+$ ion [10,13]. The target states, abbreviated by the analogous spin-1/2 states $|\downarrow\rangle$ and $|\uparrow\rangle$, are the $|F=2, m_F=-2\rangle$ and $|F=1, m_F=-1\rangle$ hyperfine states of the ${}^9\text{Be}^+ {}^2S_{1/2}$ electronic ground state. The control qubit consists of the ground and second excited states ($|0\rangle$ and $|2\rangle$) of the quantized states $|n\rangle$ of the harmonic ion motion along the trap axis or z direction. Coherent manipulation of the four qubit states and the CNOT gate action is accomplished by driving two-photon Raman transitions using two laser beams detuned from the ${}^2S_{1/2} \rightarrow {}^2P_{1/2}$, ${}^2P_{3/2}$ transitions [10,13]. The laser beams can be used to change just the spin state of the ion by driving the “carrier” transition $|\downarrow\rangle|n\rangle \leftrightarrow |\uparrow\rangle|n\rangle$ with a laser beam frequency difference $\omega_0 \sim 2\pi \times 1.25$ GHz. By tuning the frequency difference to $\omega_0 \pm \Delta n \cdot \omega_z$ (where ω_z is the harmonic oscillator frequency) both the spin state and motional level can be changed via driving the Δn th order sideband: $|\downarrow\rangle|n\rangle \leftrightarrow |\uparrow\rangle|n + \Delta n\rangle$. We refer to the “blue” sidebands for $\Delta n \geq 1$ and “red” sidebands for $\Delta n \leq -1$. In this way, any of the four qubit eigenstates ($|\downarrow\rangle|0\rangle$, $|\uparrow\rangle|0\rangle$, $|\downarrow\rangle|2\rangle$, $|\uparrow\rangle|2\rangle$) and any superposition of them can be generated from the initial state $|\downarrow\rangle|0\rangle$ that is prepared by optical pumping and laser cooling [5].

The CNOT gate is implemented by applying a single Raman laser pulse on the carrier transition. The gate action relies on tuning the laser-atom interaction by adjusting (via changing the trap strength) the relative overlap of the motional qubit state wave function with the laser field. The carrier Rabi rate for the $|2\rangle$ motional state is reduced compared to the $|0\rangle$ state because the $|2\rangle$ state has a broader spatial extent and the ion spatially averages (on a length scale comparable to the effective wavelength) over the laser field [12,16,17]. This effect is a manifestation of the wave-packet nature of the ions—we cannot obtain the observed interaction with the laser by assuming that the ions are harmonically bound point particles [18].

By adjusting the trap strength and therefore manipulating the Lamb-Dicke parameter η , the ratio of the carrier transition Rabi rates for the $|0\rangle$ and $|2\rangle$ states $\Omega_{0,0}/\Omega_{2,2} = 2/(2 - 4\eta^2 + \eta^4)$ is set to $4/3$ ($\eta = 0.359$) in the experiments reported here. Here $\Omega_{i,j}$ is the two-photon Rabi rate for the coupling $|\downarrow\rangle|i\rangle \leftrightarrow |\uparrow\rangle|j\rangle$ and η depends on the trap frequency through $\eta = \Delta k_z \sqrt{\hbar/2m\omega_z}$ where m is the ion mass and Δk_z is the wave-vector difference of the Raman laser beams along the z direction [12]. To operate the gate, the carrier transition is driven for a time t_{gate} , evolving the state amplitudes c according to $c'_{|n\rangle} = \cos(\Omega_{n,n}t_{\text{gate}})c_{|n\rangle} - i \sin(\Omega_{n,n}t_{\text{gate}})c_{|\uparrow n\rangle}$ and $c'_{|\uparrow n\rangle} = \cos(\Omega_{n,n}t_{\text{gate}})c_{|\uparrow n\rangle} - i \sin(\Omega_{n,n}t_{\text{gate}})c_{|n\rangle}$ (cf. Equation 23 of [12]). The amplitudes c are defined so that the state of the ion is given by $\sum_{n=0,2}(c_{|n\rangle}|\downarrow\rangle + c_{|\uparrow n\rangle}|\uparrow\rangle)|n\rangle$. The pulse time t_{gate} is chosen so that the $|0\rangle$ state undergoes two full Rabi cycles, or a “ 4π -pulse” ($\Omega_{0,0}t_{\text{gate}} = 2\pi$). For the same pulse time the $|2\rangle$ state experiences 1.5 Rabi cycles, or a “ 3π -pulse” ($\Omega_{2,2}t_{\text{gate}} = 1.5\pi$). Under these conditions, the target bit (spin) of the atom flips if the control bit (motional state) is in the $|2\rangle$ state and stays the same for the $|0\rangle$ state, accomplishing the CNOT gate logic (see Fig. 1). The $\pi/2$ phase acquired on the $|2\rangle$ state can be removed by an appropriate phase shift in a prior or subsequent operation, for example, in the control qubit internal-to-motional-state mapping step required for the two spin qubit case [3]. The scheme employed here is a specific case of more general possibilities outlined in [16].

A single $^9\text{Be}^+$ ion is trapped in a linear Paul trap using a combination of static and time varying electric fields to produce a three-dimensional harmonic confining potential [14]. The harmonic oscillator frequency along the trap (z) axis is set to 3.4 MHz by adjusting the static potentials

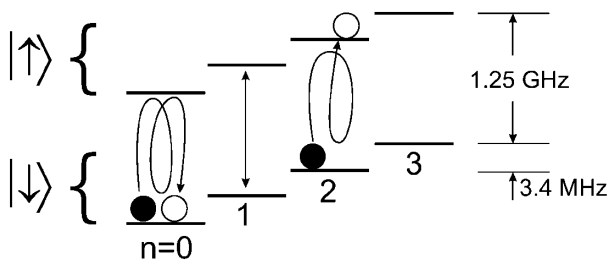


FIG. 1. Schematic of the trapped ion levels and CNOT gate operation. Shown here are the trapped ion motional levels (separated in energy by $h \times 3.4$ MHz, where h is Planck's constant) and internal spin states $|\uparrow\rangle$ and $|\downarrow\rangle$. The motional states act as the control and the internal state as the target qubit for the gate. The control qubit is composed of the ground and second excited motional states ($n = 0, 2$) along the trap axis. The CNOT gate is operated by driving the carrier transition which couples spin states with the same n . The laser-atom interaction is tuned so that an ion in the $|0\rangle$ state returns to its initial spin state while an ion in the $|2\rangle$ state toggles its spin state when the gate is driven. In the figure, filled circles represent two possible input ion eigenstates and open circles show the corresponding output state after the CNOT gate is applied.

in order to adjust η so that $\Omega_{0,0}/\Omega_{2,2} = 4/3$. State preparation and qubit manipulation are accomplished using a pair of noncollinear Raman beams [5,13]. The beams are detuned by $\sim +80$ GHz from the electronic $^2S_{1/2}$ to $^2P_{1/2}$ transition at 313 nm, and the intensity in the beams is set to give $\Omega_{0,0} = 2\pi \times 92$ kHz.

Each experiment begins by initializing the ion qubit into the $|\downarrow\rangle|0\rangle$ state with 99.9% probability using resolved-sideband Raman cooling and optical pumping [4,6,19]. The gate input state is then prepared using combinations of carrier and sideband transitions. After applying the gate, the experimental observable is the spin state of the ion which is determined through resonance fluorescence measurements [13,20]. The ion is illuminated for 200 μs by a σ^- polarized beam detuned by -10 MHz from the electronic $^2S_{1/2}$, $|\downarrow\rangle$ to $^2P_{3/2}$ ($F = 3, m_F = -3$) excited state transition. The histogram of scattered photons collected onto a photomultiplier tube is recorded for 200 experiments with identical parameters. The bright $|\downarrow\rangle$ state is distinguished from the dark $|\uparrow\rangle$ state by the difference in photon scattering rates. The probability $P_1 = \sum_n |c_{|n\rangle}|^2$ to find the ion in the $|\downarrow\rangle$ state is determined by fitting the measured fluorescence histogram to reference histograms measured from the $|\downarrow\rangle|0\rangle$ and $|\uparrow\rangle|0\rangle$ states. The fit uncertainty is typically less than 1%.

We characterize the logic gate by measuring both the logic truth table and the gate coherence. The CNOT gate truth table is determined by measuring the ion spin output state for different input eigenstates, in analogy with a classical logic gate. The measured output state for each of the logic basis states is shown in Table I. The four basis states are generated from the $|\downarrow\rangle|0\rangle$ state using combinations of carrier and sideband π pulses [5]: the $|\uparrow\rangle|0\rangle$ state is prepared from the $|\downarrow\rangle|0\rangle$ by driving a π pulse on the carrier transition, the $|\downarrow\rangle|2\rangle$ state is prepared by driving a π pulse on the first blue sideband ($\Delta n = +1$) and then the first red sideband ($\Delta n = -1$), and the $|\uparrow\rangle|2\rangle$ state is prepared by driving a π pulse on the second blue sideband ($\Delta n = +2$). The input spin state of the ion is prepared with better than 96% accuracy. After input state preparation, the CNOT gate is applied by driving the carrier transition for t_{gate} , and then the ion spin state is

TABLE I. Measured CNOT logic truth table. The measured probability that the ion is in the $|\downarrow\rangle$ state after application of the CNOT gate is shown for different input eigenstates. We observe the expected CNOT behavior where the spin state of the ion is flipped for $n = 2$ and remains unchanged for $n = 0$ (note that the probabilities do not sum to unity because these data represent the results of four separate experiments). The errors in the gate logic compared to the ideal case include errors in input state initialization.

	\downarrow	\uparrow
$n = 0$	0.989 ± 0.006	0.050 ± 0.007
$n = 2$	0.019 ± 0.007	0.968 ± 0.007

measured. For each of the basis states, we achieve at least 95% accuracy in the CNOT logic [21].

A key feature of quantum logic gates is the ability to “parallel process” superposition input states, a capability that classical logic lacks. Figure 2 shows the gate acting on the superposition input state $(1/\sqrt{2})(|\downarrow\rangle|0\rangle + |\uparrow\rangle|2\rangle)$. The input state is prepared by applying a $\pi/2$ pulse on the second blue sideband starting from the $|\downarrow\rangle|0\rangle$ state. The CNOT gate should flip the spin if the ion is in the $|2\rangle$ state, so that the expected output state is $(1/\sqrt{2})(|\downarrow\rangle|0\rangle + i|\downarrow\rangle|2\rangle)$ and the ion is always found in the $|\downarrow\rangle$ state. Figure 2 shows the measured probability to find the ion in the $|\downarrow\rangle$ state as the carrier transition is driven for an increasing period of time. The beating observed is due to the two different carrier Rabi oscillation frequencies for the $|0\rangle$ and $|2\rangle$ states. A fit of the data in Fig. 2 to a sum of two sine functions gives $\Omega_{0,0}/\Omega_{2,2} = 1.295 \pm 0.002$. Our ability to set the desired ratio $\Omega_{0,0}/\Omega_{2,2} = 4/3$ is limited in part by slow drift in ω_z caused by changing stray electric fields with spatial curvature. The accuracy of the gate logic is robust to deviations from $\Omega_{0,0}/\Omega_{2,2} = 4/3$, and, at the gate time, the ion is in the $|\downarrow\rangle$ state 98% of the time.

Measuring the population in the $|\downarrow\rangle$ state after applying the gate to a superposition input state does not determine that the CNOT gate acts coherently. To verify the gate coherence, we perform an interferometric phase measurement using the input state $(1/\sqrt{2})|\downarrow\rangle(|0\rangle + e^{i\phi}|2\rangle)$. This state is prepared from $|\downarrow\rangle|0\rangle$ by applying a $\pi/2$ pulse on the first blue sideband with a phase ϕ followed by a π pulse on the first red sideband. If the gate acts coherently

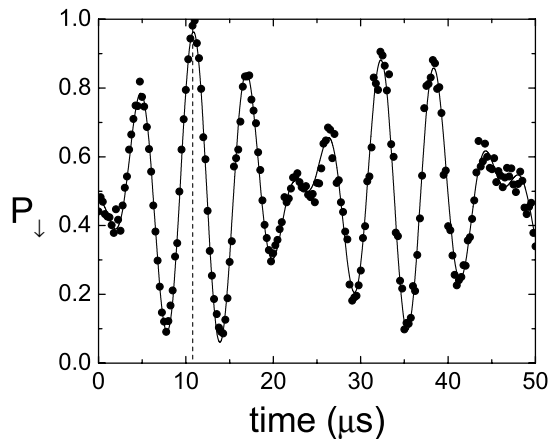


FIG. 2. CNOT gate acting on a superposition state. The input state $(1/\sqrt{2})(|\downarrow\rangle|0\rangle + |\uparrow\rangle|2\rangle)$ is prepared and then the carrier transition is driven for an increasing period of time. At the CNOT gate time t_{gate} (indicated by the dashed line), the probability P_{\downarrow} to find the ion in the $|\downarrow\rangle$ state is 98%, which is in agreement with the expected output state $(1/\sqrt{2})(|\downarrow\rangle|0\rangle + i|\downarrow\rangle|2\rangle)$. The solid line is a fit of the data to the sum of two sine functions with an exponentially decaying envelope. The decay in the Rabi oscillation contrast with a $170 \pm 10 \mu\text{s}$ time constant (as determined by the fit) is primarily due to laser intensity and magnetic field fluctuations.

on the input state, then the pure state $(1/\sqrt{2})(|\downarrow\rangle|0\rangle + ie^{i\phi}|\uparrow\rangle|2\rangle)$ is generated by the gate. Alternatively, if the gate transfers population incoherently, then the state after the gate is characterized by the mixed state density matrix $\rho = \frac{1}{2}(|\downarrow\rangle|0\rangle\langle 0|\langle\downarrow| + |\uparrow\rangle|2\rangle\langle 2|\langle\uparrow|)$. To test for the coherence, after applying the CNOT gate to the input state, a $\pi/2$ analysis pulse on the second blue sideband (with arbitrary but constant phase) is applied, and then P_{\downarrow} is measured. For coherent gate action, the final state after the analysis pulse should oscillate fully between the states $|\downarrow\rangle|0\rangle$ and $|\uparrow\rangle|2\rangle$, while incoherent gate behavior produces no dependence on ϕ . Figure 3 shows the observed oscillations in P_{\downarrow} as the phase ϕ is varied demonstrating the coherence of the gate. The lack of 100% contrast in the fringes is due to imperfections in the state and analysis pulses as well as limited gate fidelity.

A novel feature of the gate demonstrated here is the absence of level shifts introduced by the gate coupling. Other CNOT and phase gates for the trapped ion system are affected by shifts in the energy of the levels involved in the gate. These level shifts can be caused by the existence of off-resonant couplings to “spectator” levels, for example, [12,22]. If the energy spacing between levels changes when the coupling is applied, a phase error can accumulate over the course of an extended computation which then must be corrected. In the limit where the two-photon Rabi rate is small compared to the trap frequency, the two-photon energy shift ΔE for $|\downarrow\rangle|n\rangle$ and $|\uparrow\rangle|n\rangle$ caused by the sideband couplings can be expressed as

$$\Delta E(\downarrow, n) = \hbar \sum_{i \neq n, i \geq 0} \frac{1}{\omega_z} \frac{\Omega_{i,n}^2}{n - i} = \Delta E(\uparrow, n). \quad (1)$$

Here the shift ΔE is caused by the presence of off-resonant sideband couplings to higher and lower energy

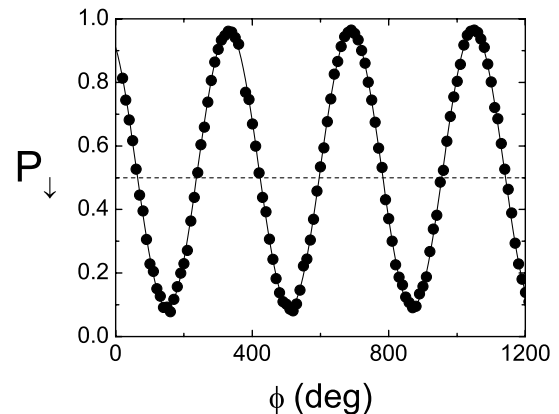


FIG. 3. Coherence measurement. To establish the CNOT gate coherence, we perform an interferometric phase measurement using the input state $(1/\sqrt{2})|\downarrow\rangle(|0\rangle + e^{i\phi}|2\rangle)$. After applying the CNOT gate and then an analysis $\pi/2$ pulse on the second blue sideband, the probability to find the ion in the $|\downarrow\rangle$ state is measured for different phases ϕ . No sensitivity to ϕ is expected if the gate acts incoherently (shown by the dashed line). The solid line shows a fit of the data to a sine function.

motional states. Pairs of coupled levels ($|\downarrow\rangle|n\rangle$ and $|\uparrow\rangle|n\rangle$) shift in energy by the same amount, so that the difference $\Delta E(|\uparrow\rangle, n) - \Delta E(|\downarrow\rangle, n)$ relevant to quantum logic operations vanishes. Physically this occurs because there are an equal number of equally detuned red and blue sideband transitions from states with the same n [23]. Equation (1) is valid only when coupling to nonresonant spectator levels can be considered as a perturbation. As $\Omega_{n,n}$ increases, the amplitudes of the spectator levels become significant so that after applying the gate information is lost to states outside the computational basis [12,21,22]. Therefore, as with the gates of Refs. [3,10], the gate speed ($\propto \Omega_{n,n}$) must be kept below the ion oscillation frequency [22].

In conclusion, using a single trapped ${}^9\text{Be}^+$ ion we have demonstrated a CNOT quantum logic gate between a motional and a spin qubit that is simplified compared to previous implementations. To perform a CNOT gate between two ions, the state of the control ion must first be mapped onto the selected motional mode, followed by a CNOT operation between the motion and target ion as in the original proposal of Cirac and Zoller [3]. However, the gate shown in this work does not require auxiliary levels, uses only a single laser pulse, and is free from level shifts caused by the gate coupling. The ability to manipulate the motional states of the ion was enabled in part by improvements in ion trap technology; the latest generation of NIST ion traps exhibits a factor of 100 reduction in the motional state heating rate [14]. With anticipated further reductions in the heating rate and improvements in system stability, the conditions for fault-tolerant computation with trapped ions appears feasible.

The authors thank Murray Barrett, David Lucas, and Andrew Steane for suggestions and comments on the manuscript. This work was supported by the National Security Agency (NSA) and Advanced Research and Development Activity (ARDA) under Contract No. MOD-717.00.

*Present address: Department of Physics, Technion, Haifa, Israel.

†Present address: NIST Optoelectronics Division, Boulder, CO.

‡Permanent address: Institute of Physics, Belgrade, Yugoslavia.

- [1] M. A. Nielsen and I. L. Chuang, *Quantum Computation and Quantum Information* (Cambridge University Press, Cambridge, U.K., 2000).
- [2] D. Bouwmeester, A. Ekert, and A. Zeilinger, *The Physics of Quantum Computation* (Springer-Verlag, Berlin, 2001).
- [3] J. I. Cirac and P. Zoller, Phys. Rev. Lett. **74**, 4091 (1995).
- [4] C. Monroe *et al.*, Phys. Rev. Lett. **75**, 4011 (1995).
- [5] D. M. Meekhof, C. Monroe, B. E. King, W. M. Itano, and D. J. Wineland, Phys. Rev. Lett. **76**, 1796 (1996).
- [6] B. E. King *et al.*, Phys. Rev. Lett. **83**, 4713 (1999).
- [7] A. Ben-Kish *et al.*, quant-ph/0208181.
- [8] H. C. Nägerl *et al.*, Phys. Rev. A **60**, 145 (1999).
- [9] Ch. Roos *et al.*, Phys. Rev. Lett. **83**, 4713 (1999).
- [10] C. Monroe *et al.*, Phys. Rev. Lett. **75**, 4714 (1995).
- [11] C. A. Sackett *et al.*, Nature (London) **404**, 256 (2000).
- [12] D. Wineland *et al.*, J. Res. Natl. Inst. Stand. Technol. **103**, 259 (1998).
- [13] C. A. Sackett, Quant. Inf. Comp. **1**, 57 (2001).
- [14] M. A. Rowe *et al.*, Quant. Inf. Comp. **4**, 257 (2002).
- [15] D. Kielpinski, C. Monroe, and D. J. Wineland, Nature (London) **417**, 709 (2002).
- [16] C. Monroe *et al.*, Phys. Rev. A **55**, R2489 (1997).
- [17] D. J. Wineland and W. M. Itano, Phys. Rev. A **20**, 1521 (1979).
- [18] A classical oscillator will show a similar suppression of its “carrier” due to the Doppler-effect-generated FM spectrum. For example, this was the basis for the conditional dynamics observed in Q. A. Turchette *et al.*, Phys. Rev. Lett. **81**, 3631 (1998). However, a quantum oscillator will exhibit a suppression due the spread of its wave packet even when it is in its ground state (Debye-Waller factor), an effect which is absent for a pointlike classical particle.
- [19] D. Leibfried *et al.*, J. Mod. Opt. **44**, 2485 (1997).
- [20] M. A. Rowe *et al.*, Nature (London) **409**, 791 (2001).
- [21] We estimate for the experimental conditions described in this manuscript that less than 0.05% of the ion population is moved outside of the $n = 0, 2$ levels by off-resonant excitation of sideband transitions. This effect can be minimized through an appropriate choice for the intensity envelope of the laser pulse.
- [22] A. Steane *et al.*, Phys. Rev. A **62**, 042305 (2000).
- [23] The level shifts introduced by the CNOT gate demonstrated in this work were analyzed in [22], but the authors did not consider the balancing contributions that cause $\Delta E(|\uparrow\rangle, n) - \Delta E(|\downarrow\rangle, n)$ to vanish.